Murine Neonatal Melanocytes Exhibit a Heightened Proliferative Response to Ultraviolet Radiation and Migrate to the Epidermal Basal Layer

Graeme J. Walker[1], Michael G. Kimlin[2], Elke Hacker[1], Sugandha Ravishankar[1], H. Konrad Muller[3,4], Friedrich Beermann[5] and Nicholas K. Hayward[1]

Melanocytes respond to UVR not only by producing melanin, but also by proliferating. This is essentially a protective response. We have studied the melanocyte proliferative response after a single UVR exposure to neonatal mice. At 3 days post-UVR in wild-type neonates we observed a marked melanocyte activation not seen in adults. Melanocytes migrated to the epidermal basal layer, their numbers peaking at 3–5 days after UVR then diminishing. They appeared to emanate from the hair follicle, migrating to the epidermis via the outer root sheath. In melanoma-prone mice with melanocyte-specific overexpression of $Hras^{G12V}$, basal layer melanocytes were increased in size and dendricity compared to UVR-treated wild-type mice. Melanocytes in mice carrying a pRb pathway cell-cycle defect (oncogenic $Cdk4^{R24C}$) did not show an enhanced response to UVR such as those carrying $Hras^{G12V}$. The exquisite sensitivity to UVR-induced proliferation and migration that characterizes neonatal mouse melanocytes may partly explain the utility of this form of exposure for inducing melanoma in mice that carry oncogenic mutations.

Journal of Investigative Dermatology (2009) **129,** 184–193; doi:10.1038/jid.2008.210; published online 17 July 2008

INTRODUCTION

Malignant melanoma (MM) development is strongly influenced by sun exposure. But MMs often appear on non-sun-exposed body sites (Whiteman *et al.*, 2003, 2006), and office workers are at higher risk than outdoor workers (Beral and Robinson, 1981; Rivers, 2004). Individuals developing MMs at anatomical sites associated with intermittent sun exposure (e.g., trunk) often also carry many nevi (Whiteman *et al.*, 2003), indicating that the innate propensity of melanocytes (MCs) to proliferate may play an underlying role in trunk lesions. UVR can induce an increase in epidermal MC numbers in human (Quevedo *et al.*, 1965; Stierner *et al.*, 1989; Scott and Haake, 1991), and mouse (Sato and Kawada, 1972; Rosdahl and Szabo, 1978; Quevedo and Fleischmann, 1980) skin, particularly after multiple exposures. There may be interindividual variation in this MC proliferative response (Stierner *et al.*, 1989; Scott and Haake, 1991). MC activation should be protective, in terms of inducing melanin synthesis. However the propensity of an individual's MCs to proliferate in response to sun damage has been suggested as a factor that may play a role in MM risk, at least in a subset of MM cases (Grichnik *et al.*, 1998; Silvers and Mintz, 1998; Rivers, 2004; Lin and Fisher, 2007).

Most mouse MM models carry mutations that upregulate the Ras/Raf/MAPK and/or Akt/PI3K pathways in MCs (*Tyr-Hras*^{G12V}, *Tyr-Nras*^{Q61K}), or in both keratinocytes and MCs (*Mt-Hgf/Sf*, *Grm1*; *Mt-Ret*) (reviewed in Walker and Hayward, 2002). Such genetic modifications can induce melanocytosis and MM, with UVR exposure generally increasing penetrance and reducing age of onset. Penetrance is increased if transgenics are crossed with mice carrying p53 (Bardeesy *et al.*, 2001; Kannan *et al.*, 2003) or pRb (Recio *et al.*, 2002; Kannan *et al.*, 2003; Ackermann *et al.*, 2005; Hacker *et al.*, 2006) pathway defects.

In *Hgf/Sf* transgenic mice a single neonatal UVR exposure effectively induces MM, whereas adult doses do not (Noonan *et al.*, 2001). This process appears to be driven by UVB, as neonatal UVA was ineffective at inducing MM (De Fabo *et al.*, 2004). The action spectrum for non-MM skin carcinogenesis in mice peaks at 293 nm (de Gruijl *et al.*, 1993), squarely within the UVB band. However UVA1 (340–400 nm) has also been suggested to be important in MM development. Whereas UVB is absorbed strongly by DNA, UVA is absorbed only weakly, and may induce damage indirectly

[1]*Oncogenomic Laboratory, Queensland Institute of Medical Research, Herston, Queensland, Australia;* [2]*Australian Sun and Health Research Laboratory, Queensland University of Technology, Kelvin Grove, Queensland, Australia;* [3]*School of Medicine, University of Tasmania, Hobart, Tasmania, Australia;* [4]*Pathology Queensland, Royal Brisbane and Women's Hospital, Herston, Queensland, Australia and* [5]*Swiss Institute for Experimental Cancer Research, Ecole Polytechnique Fédérale de Lausanne, Epalinges, Switzerland*

Correspondence: Dr Graeme J Walker, Oncogenomic Laboratory, Queensland Institute of Medical Research, 300 Herston Road, Herston, Qld 4006, Australia. E-mail: Graeme.Walker@qimr.edu.au

Abbreviations: CPD, cyclobutane pyrimidine dimer; MC, melanocyte; MM, malignant melanoma; ORS, outer root sheath; Trp, tyrosinase-related protein; wt, wild type

Received 17 December 2007; revised 3 June 2008; accepted 5 June 2008; published online 17 July 2008

by photosensitizing other molecules by which it is absorbed, resulting in free radical formation. A single UVA dose does not induce MC proliferation in adult mice, which UVB does effectively (van Schanke *et al.*, 2005).

The reason for the sensitivity of murine neonatal, but not adult MCs, to UVR-induced transformation is unclear (Wolnicka-Glubisz and Noonan, 2006). As neonatal mice have a defective inflammatory response to UVR (Wolnicka-Glubisz *et al.*, 2007), it may involve the relative immaturity of the immune system. An alternative hypothesis involves the location of MCs in the skin. In adult mice, MCs are restricted to hair bulbs (except in certain anatomical locations such as the tail and ears), rather than the epidermis as in humans. In neonates, MCs are transiently within the epidermis, but migrate into hair bulbs before postnatal day 10 (Hirobe, 1984). Thus UVR treatment of neonates probably results in damaged epidermal MCs, whereas in adult mice this would not be the case.

We have shown that mice carrying MC-specific activation of $Hras^{G12V}$ (*Tpras*) are highly MM prone after a single neonatal but not chronic adult UVR exposure (Broome Powell *et al.*, 1999; Hacker *et al.*, 2005). MMs were small and *in situ*. When these mice were also homozygous for the Cdk4 mutation (R24C) that makes the kinase insensitive to p16Ink4a inhibition (Rane *et al.*, 1999), neonatal UVR decreased age of onset and increased tumor aggressiveness (Hacker *et al.*, 2006). As UVR is known to activate MCs *in vivo*, we hypothesized that this response may be exacerbated in neonatal mice. We examined UVR-induced MC proliferation in *Tpras* (Broome Powell *et al.*, 1999), $Tyr\text{-}Nras^{Q61K}$ (*Tyr-Nras*) (Ackermann *et al.*, 2005) and/or oncogenic Cdk4 (Rane *et al.*, 1999) mice, to determine whether it may be a factor in neonatal UVR-induced melanomagenesis, and whether UVR exposure has a similar effect on MCs carrying activation of *NRAS*, given that *NRAS* mutations are more common than *HRAS* mutations in human MM. We collected skin from UVR-treated mice and used immunofluorescence to detect MCs staining for Trp1 (a MC marker) and/or Trp2 (a marker for both MCs and melanoblasts); and Ki-67, which stains cycling cells (Gerdes *et al.*, 1984). We chose to study dorsal skin as this is where the great majority of UVR-induced MMs develop in the murine models we have studied (Hacker *et al.*, 2006).

RESULTS

Melanocyte activation in wild-type mice

We often noted retarded hair growth in pups for a few days after neonatal UVR treatment (Figure 1a), after which the hair grows normally. At 24 hours post-UVR, we tended to observe few Ki-67-positive proliferating cells and isolated areas of seemingly disorganized epidermis in exposed skin (Figure 1b). This contrasted with the well-demarcated epidermis, with proliferating basal cells, in shielded skin (Figure 1b, right panels). Notably, at 24 hours after UVR no Trp1 or Trp2-staining MCs were visible in the damaged epidermis, they were only located within hair bulbs (not shown). Surprisingly, at day 3 post-UVR, we observed MCs in the epidermal basal layer (Figure 1c) in the UVR exposed but not the shielded side of the animal. Importantly, in adult wild-type (wt) dorsal skin after a single exposure of equal intensity, MCs did not appear at the basal layer (Figures 1d and 2a). In the neonates, the attraction of MCs to the basal layer in neonates (not observed at 24 hours postneonatal UVR) seemed to correlate with increased basal keratinocyte proliferation, observed at 5 days post-UVR in exposed and not shielded skin (Figure 1c). Comparison of MC number in the epidermis at various time points (including those preexisting at postnatal day 3, P3, at the time of neonatal UVR) indicates that epidermal basal MC density is extremely low at 1 day after UVR, peaks at 3–5 days, along with increasing basal keratinocyte proliferation, then gradually diminishes (Figure 2b), presumably after the damaged epidermis is renewed.

Melanocyte activation in Ras transgenics

Table 1 details the spontaneous and UVR-induced melanoma susceptibility of the mouse strains used in this study. MCs migrating to the basal layer in MM-prone *Tpras* and $Tyr\text{-}Nras^{Q61K}$ mice tended to be larger and more dendritic (for example, Figure 1e) than those in wt UVR-treated skin. Dendritic processes were often multipolar, compared to the generally bipolar wt basal MCs. The Ras-expressing MCs appeared anchored on the basal membrane, with dendrites reaching up toward the suprabasal epidermis (Figure 1e and f), as is normally seen in human skin. In isolated pockets, MCs appeared to line nearly the whole of the basal layer (Figure 1f), although the density of infiltration varied along a particular skin section. This phenomenon was not seen in UVR-treated wt skin, where basal MCs were separated, and not in chains as in Figure 1f. Extra-follicular dermal MCs in the shielded dorsal skin of *Tpras* (Figure 1f) and *Tyr-Nras* mice (Ackermann *et al.*, 2005) are part of the phenotype of these transgenics due to constitutive Ras activation. These cells lie close to, but beneath, the dermal–epidermal junction, with dendrites following the curve of the basal layer. Only in UVR-exposed skin do MCs become resident in the basal layer.

Despite qualitative differences in the size and dendricity between the wt and Ras-expressing basal MCs, this was not always accompanied by significant differences in cell number. When basal MC density was assessed, (Figure 2c), there was a trend for greater numbers (than wt) in genotypes carrying a *Ras* transgene, only reaching statistical significance for *Tyr-Nras* at 3 days post-UVR. We observed no difference in UVR-induced basal MC numbers between mice carrying combined Cdk4 and Ras mutations from those carrying Ras only (Figure 2c), or between wt and $Cdk4^{R24C/R24C}$ mice (not shown). In all genotypes, basal MC density was decreased by 2 weeks post-UVR (Figure 2d). Unlike adult wt mice, where we observed no basal MCs post-UVR, an equivalent dose to 8-week-old *Tpras* mice resulted in the appearance of small numbers of basal MCs (Figures 1g and 2a). However basal MC density after UVR was significantly lower in adult *Tpras* skin than in neonatal *Tpras* skin (Figure 2a), and the adult basal MCs were generally smaller.

UVR-induced melanocyte proliferation in melanoma-prone mice

We sought to determine the proportion of UVR-activated basal MCs that stained for both Trp1 and Ki-67 (Figure 3a).

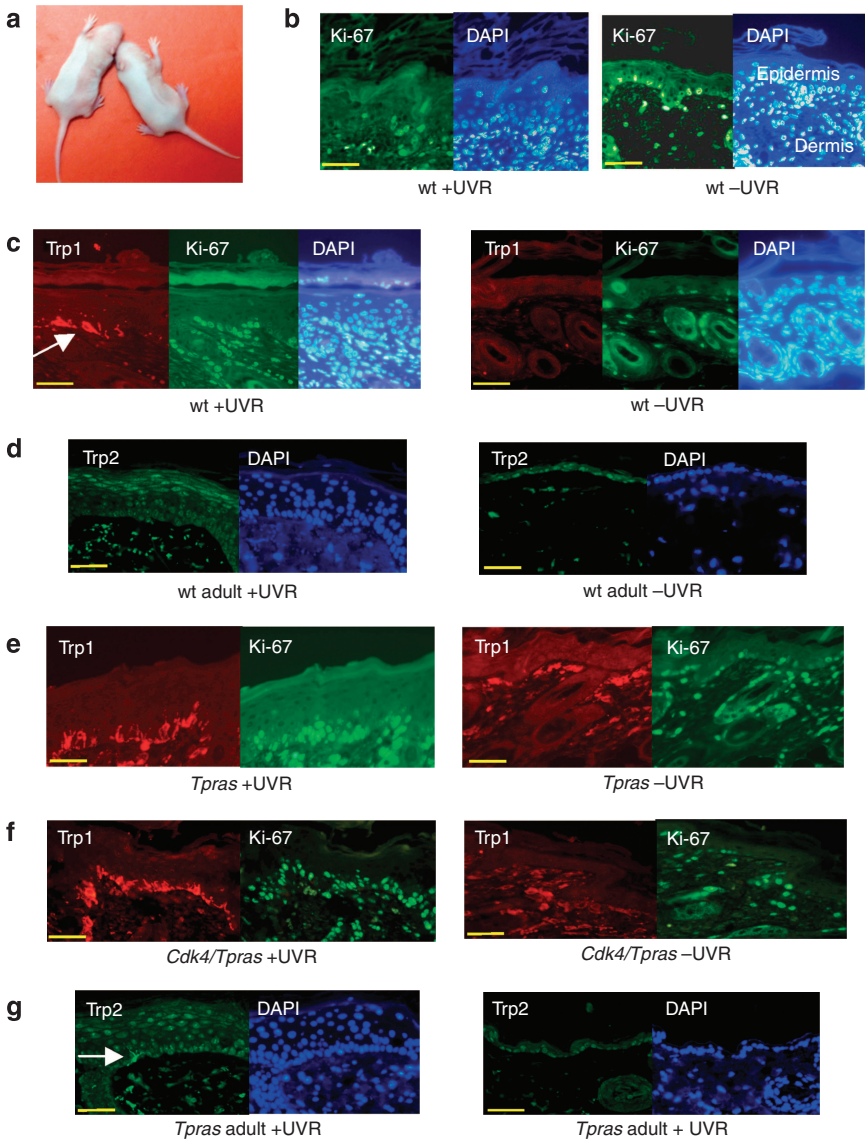

Figure 1. UVR-induced melanocyte proliferation. (**a**) Inhibition of hair growth 3 days postneonatal UVR (P6). At UVR exposure, the left side of the animal was shielded with UVR-blocking tape. (**b**) UVR-exposed wt dorsal skin 24 hours post-exposure (P4), showing low levels of proliferating basal keratinocytes, giving the appearance of a disorganized epidermis. Sections were stained for proliferating cells (Ki-67, green) and nuclei (DAPI, blue). Right panel shows shielded skin of the same mouse, with proliferating keratinocytes (green) along a sharply defined basal layer; (**c**) 5 days post-UVR (P8). Trp1-staining (red) dendritic MCs can be seen residing in the basal layer in UVR-exposed, and not the shielded side (right panels). Ki-67 staining along the basal layer is greatly increased and epidermis thickened. Neither can be observed in shielded skin, with MCs strictly limited to hair follicles. (**d**) Shaved UVR-treated skin (4 days after UVR) from an 8-week-old wt mouse. Right panels show nonshaved (shielded) skin from the same animal. Dermal fluorescence in UVR-treated skin is due to background fluorescence of red blood cells. (**e**) UVR-exposed (left) and shielded (right) *Tpras* skin, showing dendritic MCs in the basal layer at 5 days post-UVR (P8). Dendrites extend up into the epidermis, as in human skin. Note dermal MCs in both UVR-treated and shielded *Tpras* skin. (**f**) UVR-exposed (left) and shielded (right) skin of $Cdk4^{R24C/R24C}$/*Tpras* mouse at 5 days post-UVR (P8). Isolated aggregations of MCs can be observed along the basal layer after neonatal UVR, but not in shielded skin. (**g**) Shaved and UVR-treated skin (4 days after UVR) from an 8-week-old *Tpras* mouse. Arrow indicates an epidermal basal layer MC. The right panels show nonshaved (shielded) skin from the same animal. Green staining in the dermis is nonspecific background fluorescence. Scale bar = 100 μM.

At least 24% (up to 40% in $Cdk4^{R24C/R24C}$/*Tpras* mice) of these cells were proliferating. Thus, in the epidermis MCs are highly activated and appear capable of subsequent expansion. This further underlines a predictable, but pivotal difference between MCs in neonatal versus adult mice, their propensity for proliferation and activation post-UVR. We also assessed the dermal population of MCs in the *Tpras* and $Cdk4^{R24C/R24C}$/*Tpras* animals. In total, 36–40% (Figure 3b) of these dermal MCs stained for Ki-67, indicative of the hyperproliferative phenotype induced by MC-specific expression of $Hras^{G12V}$. However, we saw no difference in the proportion of these cells proliferating after neonatal UVR. Thus untreated Ras-expressing dermal MCs are also characterized by high levels of proliferation that was not measurably increased by neonatal UVR. In terms of MC localization within the skin, their appearance in the basal layer is the most prominent response to neonatal UVR in both wt and MM-prone transgenic mice.

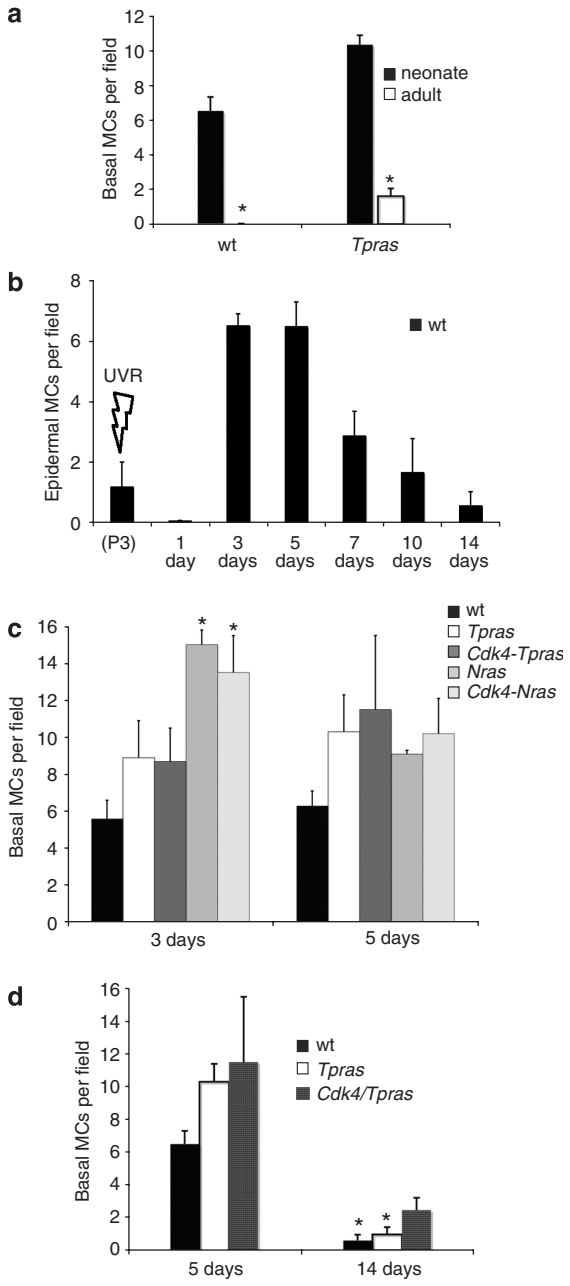

Figure 2. UVR-induced basal melanocyte number in different strains. Mean basal MC number (±SEM) per ×40 field over the length of each section (over ~20–25 fields per section) is plotted against days postneonatal UVR. (**a**) Comparison of basal MC count after neonatal UVR in neonates and adults (wt and *Tpras*, respectively), $n=4$ for each time point. *Mann–Whitney *U*-test $P<0.05$. (**b**) Epidermal MC density for wt mice plotted at P3 (preexisting MCs) and from days1–14 after neonatal UVR. (**c**) wt mice compared to *Tpras* and *Tyr-Nras* transgenics and/or compound genotypes with $Cdk4^{R24C}$. Sections were analyzed from at least 3 different mice (except for $Cdk4^{R24C/R24C}$/*Tpras* at 5 days, $n=2$), from at least 2 different litters). *Mann–Whitney *U*-test $P<0.05$. (**d**) Basal MC count at 5 and 14 days post-UVR ($n\geqslant 30$. Some MCs remain in the basal layer for up to 2 weeks postneonatal UVR. Mean counts for wt and *Tpras* are significantly lower at 14 days than at 5 days post-UVR (*Mann–Whitney *U*-test $P<0.05$). For *Tyr-Nras* $P=0.077$.

DNA repair of damaged melanocytes in *Tpras* and $Cdk4^{R24C/R24C}$/*Tpras* mice

To determine whether UVR-induced MC proliferation in the transgenic mice may inhibit DNA repair, we assessed removal of cyclobutane pyrimidine dimers (CPDs) after neonatal UVR. If *Tpas* or $Cdk4^{R24C/R24C}$/*Tpras* MCs were defective in DNA damage repair, we would expect to see repair substantially completed after 3–4 days in keratinocytes (Tron *et al.*, 1998; Figure S1a), but not in MCs. By double-label immunofluorescence staining we detected CPDs in the epidermis and upper dermis (Figure 3c). Overlay of Trp1 and CPD staining revealed many damaged MC nuclei after neonatal UVR (Figure 3d). Although damaged MCs and keratinocytes could be observed at 48 hours post-UVR, CPDs were cleared in both cell types by 5 days (Figure 3d). Thus, we found no evidence that CPDs were repaired more slowly in MCs than keratinocytes. Notably, neither UVR-activated basal layer MCs, or those in the dermis, showed evidence of retaining CPDs. We cannot rule out the possibility that MCs may not have repaired some DNA lesions, but there is no indication of a significant repair defect in these hyperproliferating mutant MCs *in vivo*. Removal of CPDs appears to be substantially completed by the time of maximum MC migration to the epidermal basal layer.

Effect of UVA on melanocyte proliferation in neonatal mice

On basis of the data of De Fabo *et al.* (2004), we predicted that if epidermal MC proliferation/activation is important for MM induction, one would not expect UVA to increase epidermal MC numbers. We exposed wt mice to a single neonatal UVA dose of 81 kJ m^{-2}. In contrast to UVB-treated littermates, we did not observe any MCs in the epidermal basal layer at 3 or 6 days post-UVR (Figure 4). In the UVA-treated skin, we did not observe increased Ki-67-staining basal cells, or epidermal thickening. Thus in neonatal mice UVR-induced MC proliferation is largely driven by UVB photoproduct formation.

Origin of UVR-activated basal melanocytes in mice

Insertion into the epidermal basal layer of preexisting epidermal MCs. As MCs are present in the epidermis in neonates, and not in adult mice, we hypothesized that these cells may amplify and insert into the basal layer after neonatal UVR. We stained skin from untreated wt mice at P1-P10 for Trp1 and Trp2. From P1–10, epidermal MCs (mainly suprabasal, Figure 5a) peak, then diminish in number (Figure 5b) as they migrate downward into the developing hair follicle via the outer root sheath (ORS). They are undetectable in the epidermis by P10 (in accord with Hirobe, 1984). At P3, the time of neonatal UVR, the density of these suprabasal MCs varied between genotypes (Figure 5c), with the *Tpras* animals having surprisingly few, but *Tyr-Nras* mice having a relatively high density. Both Ras genotypes exhibited comparable basal MC numbers post-UVR. The fold increase for different genotypes was wt (5.6), *Tpras* (36.8), and *Nras* (3.8). Thus the numbers of preexisting suprabasal epidermal MCs does not correlate well with the subsequent basal MC counts post-UVR. The density of preexisting extra-follicular

Table 1. Melanoma susceptibility of single and compound transgenic strains

	MM penetrance at 1 year		Average age-of-onset	
Strain	**Spontaneous**	**UVR induced**	**Spontaneous**	**UVR induced**
Tpras	0%[1]	57%[1]	—[1]	35 weeks[1]
Tyr-Nras^{Q61K}	15%[2]	ND	50 weeks[2]	ND
Cdk4$^{R24/R24C}$*/Tpras*	58%[3]	83%[3]	36 weeks[3]	23 weeks[3]
Cdk4$^{R24/R24C}$*/Tyr-Nras*^{Q61K}	ND	ND	ND	ND

Abbreviations: MM, malignant melanoma; ND, not done.
We did not include wt mice as they do not develop MM after neonatal or repeated adult UVR. [1]Hacker *et al.*, 2005.
[2]Ackermann *et al.*, 2005.[3]Hacker *et al.*, 2006.

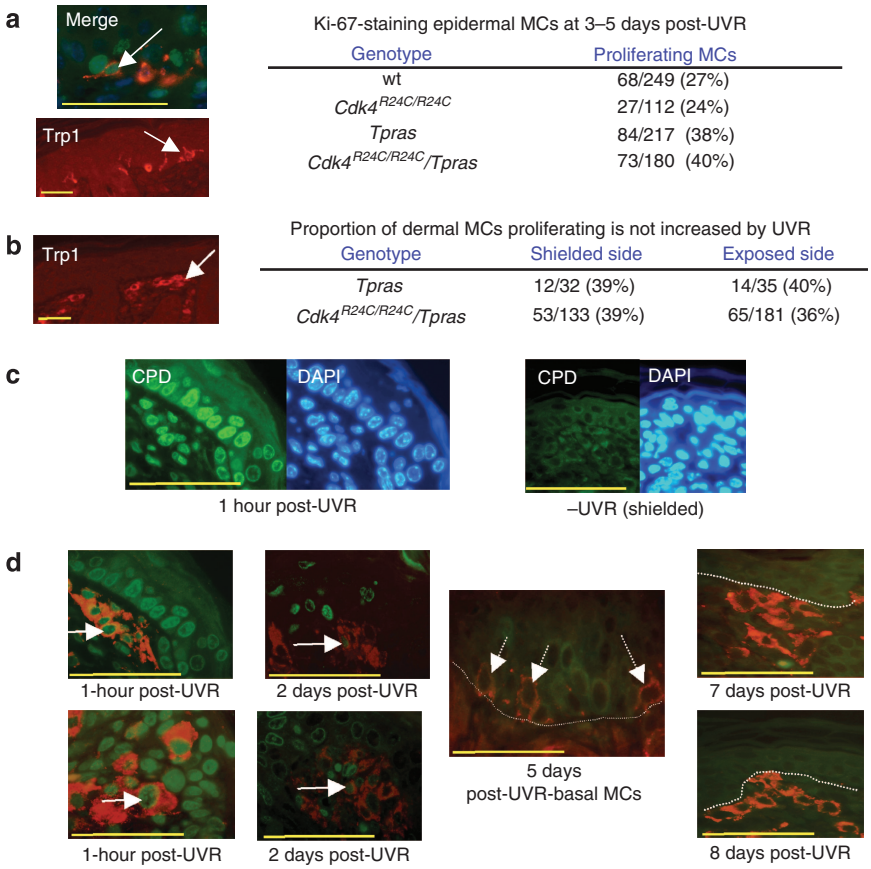

Figure 3. Proliferation and DNA repair capability of MCs post-UVR. (**a**) Top panel shows overlay of Trp1 and Ki-67 staining (indicated by an arrow). Lower panel shows Trp1-staining basal layer MCs post-UVR. Table shows the proportion of these UVR-activated basal MCs proliferating. (**b**) The proportion of dermal MCs (indicated by an arrow) proliferating in UVR-treated and shielded *Tpras* and *Cdk4*$^{R24C/R24C}$*/Tpras* skin. (**c**) Anti-CPD monoclonal antibody detects dimers in UVR-exposed skin (left panel) but not shielded skin from the same animal (right panel). Mouse strain, *Cdk4*$^{R24C/R24C}$*/Tpras*. Trp1 stain not included. (**d**) Overlay of Trp1 (red) and CPD (green) staining post-UVR. Mouse strain-*Cdk4*$^{R24C/R24C}$*/Tpras* in all panels. White arrows show DNA-damaged MC nuclei at 1 hour post-UVR, with decreased intensity at 2 days post-UVR. After 5, 6, and 8 days post-UVR (right panels), no CPDs can be detected in either MCs or adjacent keratinocytes. Dermo-epidermal junction is marked by a dotted white line. The 5 days time point shows CPD-negative basal MCs (arrows with dotted stems). The 7 and 8 days time points show CPD-negative dermal MCs. Scale bar = 100 μM.

dermal MCs also varies between genotypes (Hacker *et al.*, 2005; Figure S1b; shown schematically in Figure 5e). Thus, we cannot infer from differences in preexisting MC density whether preexisting epidermal and/or interfollicular dermal MCs may expand and insert into the basal layer after UVR. The relative role of each MC population may depend on the genotype-determined proliferative response of MCs to UVR, or alternatively, all MC populations may be attracted to the epidermal basal layer after UVR. Despite the different preexisting MC populations, all genotypes have in common the appearance of MCs in the basal layer after neonatal UVR.

Migration from hair follicles. An alternative scenario, based on our observations, is a migratory model, with MCs

emanating from the hair follicle. At the time of maximum basal MC numbers, we observed Trp1/2-staining dendritic MCs within the ORS in UVR-exposed wt skin (Figure 5f and h), but not in shielded skin from the same animal (Figure 5g and i).

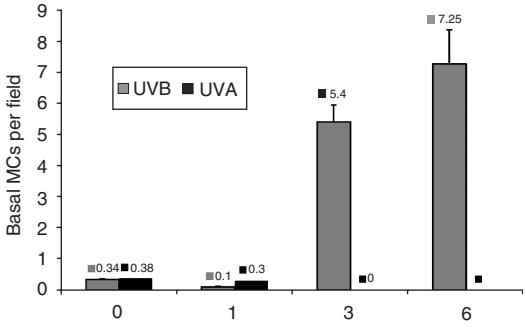

Figure 4. Lack of MC migration to the epidermis after neonatal UVA. Two wt neonatal mouse litters were analyzed, with half of each litter exposed to 5.9 kJ m^{-2} UVB and the remaining littermates to 81.3 kJ m^{-2} UVA. The average number of basal MCs (± SEM) is plotted against time post-UVA and UVB. MCs appeared in the epidermal basal layer only in UVB-exposed mice.

Here we concentrated on wt mice only, because in the Ras models we cannot rule out direct insertion of extra-follicular MCs into the ORS (at P3 wt mice have few, if any extra-follicular dermal MCs, Figure S1b). With hair growth retarded for a few days postneonatal UVR (Figure 1a), we observed follicles in various stages of maturation at 3–5 days post-UVR. In immature follicles, we saw MCs located along the descending hair follicle epithelium post-UVR. However, in well-developed follicles, by 5–6 days post-UVR MCs were nearly always seen in the follicular infundibulum and in the adjacent interfollicular epidermal basal layer (see Figure 5j and k), and only very rarely below the bulge region. This is consistent with a vertical (upward) migration of MCs toward the epidermis via the ORS. Although both the *Tpras* and *Tyr-Nras* mice harbor preexisting dermal MC populations, in both models MCs also appear in the ORS after UVR exposure (Figure S1c).

DISCUSSION

Neonatal UVR exposure has become *de rigueur* for inducing MMs in mice. We have examined mouse dorsal skin after

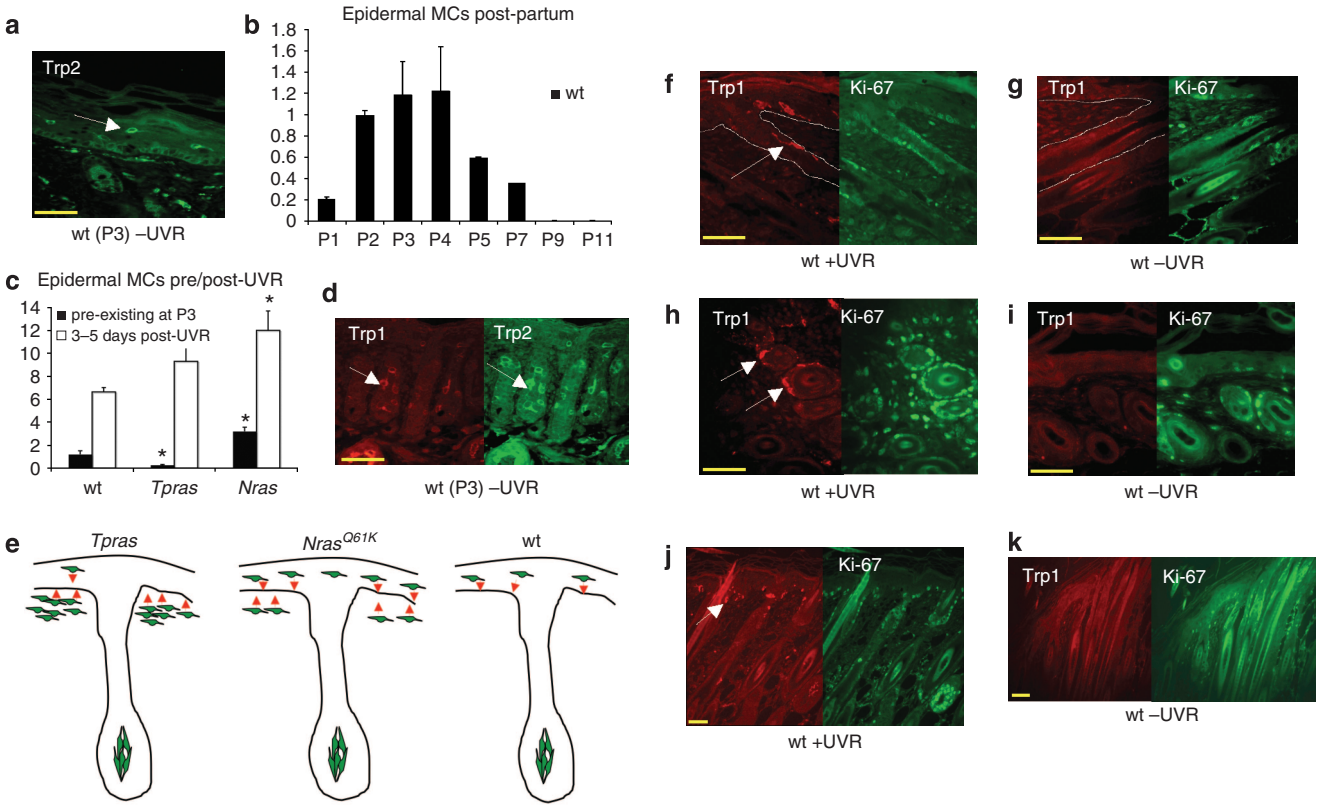

Figure 5. Migration of melanocytes pre- and post-UVR. (**a**) Untreated wt mouse at P3, showing a Trp2-staining MC in the suprabasal epidermis (arrow). (**b**) Suprabasal epidermal MC count in untreated wt mice plotted against day postpartum. (**c**) Genotype comparison of suprabasal MC number at P3 to basal layer MC count at 3–5 days post-UVR. Asterisk (*) denotes significantly different wt counts (Mann–Whitney *U*-test $P<0.05$). The difference between wt and *Tpras* at P3, $P<0.01$ (**d**) Trp1 (red) and Trp2 (green). Arrows indicate MCs in untreated skin at P3 descending from the epidermis into the developing follicle via the ORS. All MCs express both Trp1 and Trp2. (**e**) Schematic representation of MC populations present in *Tpras, Tyr-Nras,* and wt mice at P3. (**f**) Longitudinal section of wt skin at 3 days post-UVR. Arrow denotes Trp1-staining MC in the ORS. ORS and epidermal basal layer delineated by a dotted line. (**g**) Shielded side of the same animal. No MCs are visible in the ORS. (**h**) Cross-section of hair follicles at 3 days post-UVR showing MCs in the ORS. (**i**). Shielded side of animal. (**j**) Lower power image of skin 6 days after neonatal UVR. White arrows denote unfundibular and ORS MCs, and yellow arrow a rare MC lower in the ORS. (**k**) Shielded side of the animal. Scale bar = 100 μm.

neonatal UVR exposure and observed a remarkable propensity for neonatal MCs to migrate to the basal layer of the epidermis. For wt mice this migration was specific to the neonatal period, as it did not occur in adult wt mice treated with an equivalent single UVR dose, in accordance with the conclusions of others (Jimbow and Uesugi, 1982; Noonan *et al.*, 2000; van Schanke *et al.*, 2005). In addition, based on Ki-67 positivity, a much higher proportion of MCs are actively cycling in UVR-treated neonatal skin (from 24 to 40%; Figure 3a) compared to those in wt adult skin after a single exposure (less than 1%; van Schanke *et al.*, 2005). Thus UVR-activated neonatal basal layer MCs are highly proliferative and capable of further expansion, and developmental age is pivotal in determining their propensity to proliferate and migrate after UVR. This has also been reported in wound-healing experiments with mice (Hirobe, 1988). After neonatal wounding, MCs migrate to the healing epidermis, their numbers reach a maximum at 3 days postwounding, then decrease, reminiscent of our observations following neonatal UVR exposure. MC proliferation was maximal with wounding at P1.5, at later ages the effect decreased and it did not occur in 60-day-old mice (Hirobe, 1988).

MC activation after neonatal UVR was exacerbated in mice carrying MC-specific oncogenic $Hras^{G12V}$ or $Nras^{Q61K}$ mutations. The mutant MCs were increased in number in the basal layer over wt levels and were often multidendritic, whereas those in wt mice tended to be bipolar. The dorsal epidermis in the MM-prone animals at 3–5 days postneonatal UVR (Figure 1f) looks remarkably similar to human epidermis, with dendritic MCs sitting on the basement membrane and dendrites extending up into the epidermis. The hyperactivation of mutant MCs in the MM-prone mice after neonatal UVR led us to ponder whether this MC response is purely protective, or whether it may be involved in MM initiation. One simple test was to expose neonatal mice to UVA, which does not initiate MM in the albino *Mt-Hgf* model (De Fabo *et al.*, 2004). We observed no MC proliferation after UVA exposure, indicating that the same type of UVR-induced damage that induces MC migration also induces MM. This is consistent with the data of van Schanke *et al.* (2005), where UVA did not increase MC proliferation in adult mice, even after a single dose of up to $1300\,kJ\,m^{-2}$. We also tested the capacity of the mutant MCs to repair UVB-induced DNA damage. We found no evidence that they could not repair pyrimidine dimers as well as adjacent cells in their microenvironment, although we cannot rule out a role for other types of DNA damage, including oxidative damage, inhibition of which can delay age of MM onset in some models (Cotter *et al.*, 2007). We hypothesize that the presence of highly activated MCs in an environment of defective inflammatory response to UVR in neonates (Wolnicka-Glubisz *et al.*, 2007) may at least partially explain the utility of this form of radiation exposure in inducing MM in genetically modified mice. Our results support this hypothesis, but further experiments will be needed to confirm this possibility. Part of the excessive MC activation in our MM-prone models could result from increased Ras transgene expression due to UVR-induced factors binding to the exogenous tyrosinase gene promoter. This does not alter the proposition that neonatal UVR may be pivotal in placing some MCs into a hyperactive state, although they need concomitant Ras activation for transformation.

We previously showed that $Hras^{G12V}$ alone is sufficient, in cooperation with neonatal UVR, to induce MM, whereas the combination of $Cdk4^{R24C/R24C}$ and $Hras^{G12V}$ increases penetrance, with the lesions being larger and more aggressive (Hacker *et al.*, 2006). Surprisingly, the presence of an activating Cdk4 (R24C) mutation did not enhance UVR-induced MC migration. This indicates that $Hras^{G12V}$ appears to be driving MC proliferation and the initiation of MM after neonatal UVR, whereas the Cdk4 mutation either exacerbates the initiation process, or comes into play once an MC has overcome a transformation threshold.

In addition to the appearance of MCs in the epidermal basal layer, the most striking feature of UVR-treated skin in wt neonatal mice is the appearance of dendritic MCs in the ORS (Figure 5f, h and j). Treatment with chronic UVR or DNA damaging agents can also stimulate MCs to invade the epidermis via the ORS in adult mouse (Quevedo and McTague, 1963; Sharov *et al.*, 2003) and human (Staricco and Miller-Milinska, 1962) skin. Our observations before and after UVR in wt neonates suggest that just as neonatal MCs normally migrate downward into the developing hair follicle (Figure 5d, Peters *et al.*, 2002), after UVR exposure they appear to migrate upward, via the ORS, and by 6 days after neonatal UVR they are mostly seen in the infundibula region and the epidermal basal layer (Figure 5f–k). This is consistent with activation and subsequent expansion of bulge MC stem cells by UVR. These stem cells can resupply both the hair bulb and epidermis with MCs when appropriately stimulated (Nishimura *et al.*, 2002). The presence of other MC precursors, not expressing pigmentation-related antigens, has been proposed in murine (Jimbow and Uesugi, 1982; Kawaguchi *et al.*, 2001) and human epidermis (Grichnik *et al.*, 1996; Horikawa *et al.*, 1996). Although activation of such MCs by UVR cannot be ruled out, epidermal grafting experiments in animals and humans indicate that MCs can migrate vertically, via the ORS, and horizontally, through the interfollicular epidermis (Billingham and Silvers, 1970; Horikawa *et al.*, 1999; Nishimura *et al.*, 2002; Yonetani *et al.*, 2008). This ''pigment-spreading'' phenomenon is explained only by MC migration, not by activation of preexisting MCs. Whether the UVR-activated epidermal basal MCs in our study originate from activation, expansion, and migration of an ORS MC population, or insertion into the basal layer of another MC population(s), remains to be determined.

Why might neonatal MCs be so sensitive to UVR-induced proliferation and transformation? Normally, MC stem cells are activated cyclically, at anagen, to resupply the follicle. However, in neonatal mice the first hair bulbs are not supplied by MC stem cells, but by MCs that are migrating from the epidermis, in an environment of hair growth stimulus, downward into the bulb (Peters *et al.*, 2002; Mak *et al.*, 2006). Thus at P3, the time of neonatal UVR exposure,

MCs are essentially in a unique developmental window when their fate is being determined—they will migrate either into the bulge niche (Nishimura *et al.*, 2002), or the hair bulb (Peters *et al.*, 2002). Whether these MCs simply reverse their trajectory, under a ''wound'' stimulus (from UVR), or whether MC stem cells expand after UVR exposure is a fascinating question, and we are performing further experiments to try to elucidate the answer.

It is well known after epidermal MC density in the basal layer can increase after UVR exposure, a response conserved even in hairy-skinned animals that do not have a great need for tanning. In neonatal mice, the appearance of basal MCs coincides with proliferating basal keratinocytes (Figure 1c and e), in a response likely to be driven by keratinocyte-derived factors (Hirobe, 2004; Lin and Fisher, 2007). However, keratinocyte proliferation alone cannot explain the attraction of MCs to the basal layer, as UVR-treated adult wt mice show significant epidermal hyperproliferation after UVR, but no MCs migrate to the basal layer (Figure 1d). It will be interesting to determine which keratinocyte-to-MC signaling pathway(s) is important for inducing MC migration after neonatal UVR, and which innate characteristics of neonatal MCs make them particularly sensitive to these signals. MC activation in humans after sun exposure is a protective response, helping to increase melanin production, enhancing DNA repair, and inhibiting apoptosis of MCs (reviewed in Abdel-Malek *et al.*, 2008). Whether genetic variation in humans that augment the response of an individual's MCs to UVR could increase susceptibility to a particular pathway of MM development (as suggested by Whiteman *et al.*, 2003, and Rivers, 2004) remains to be determined.

MATERIALS AND METHODS

Mouse melanoma models

Mouse models and genotyping have been previously described: *Cdk4*^{R24C} (Rane *et al.*, 1999), *Tyr-Hras*^{G12V} (Broome Powell *et al.*, 1999), and *Tyr-Nras*^{Q61K} (Ackermann *et al.*, 2005). Mice were bred for at least three generations onto a friend virus B-type background. Wild-type mice were littermate controls not carrying a Cdk4 or oncogene Ras mutation. Experiments were undertaken with institute animal ethics approval A98004M.

UVR treatments

Pups (3-day-old) were given a 20 minutes exposure to UVB from a bank of six cellulose acetate-filtered Phillips TL100W 12RS UVB lamps (Total UVB dose, 5.9 kJ m^{-2}, or an erythemally weighted dose of 1.8 kJ m^{-2}). UVB dose was measured using a Solar Light (Glenside, PA) PMA2100 radiometer with either a PMA2101 detector to measure biologically weighted UVB or a PMA2106 detector to measure non-weighted UVB. The reason for the use of this dose of UVB is historical. Comparable doses of UVB effectively inducing MM in genetically modified mice (for example, Noonan *et al.*, 2001), probably in a dose-dependent manner (De Fabo *et al.*, 2004). Each pup was placed into a well of a six-well tissue culture plate for the treatment, to prevent them huddling and screening each other from the UVR. Animals were killed at 4 days post-UVR and a portion of exposed skin excised. One side of selected litters was shielded with black tape to generate untreated skin for the same mouse. Three Mylar-filtered Phillips TLK40W/05 UVA lamps were used for UVA exposures. The peak output is at 365 nm, a mercury line (see Figure S1d for spectral output). Mice were exposed to 81.3 kJ m^{-2} of UVA, with pups placed 6.5 cm from the lamps for 50 minutes. For adult exposures, a portion of dorsal skin was shaved before the exposure of 8-week-old mice to the same UVB dose. Controls were shaved mice not exposed to UVR, and nonshaved (shielded) skin from the UVR-treated animal.

Dual-label immunofluorescence

Pups were killed with CO_2 and a section of dorsal skin was excised. Sections (3–4 m) were dewaxed and antigen retrieval was performed using the Dako pH-6 system (Dako, Eli, UK) at 125 °C for 5 minutes. Sections were blocked with 1% BSA and incubated with rat monoclonal anti-Ki-67 (Dako) at 5 °C overnight. After washing, biotinylated donkey anti-rat (Jackson ImmunoResearch Laboratories, West Grove, PA) antibody was applied (at 1:300 dilution) for 1 hour, followed by washing, and incubation with FITC-labeled streptavidin (1:300) for 1 hour. The second primary antibody (anti-Trp1) was applied (1:300) for 1 hour. Rhodamine-labeled donkey anti-rabbit (Jackson ImmunoResearch Laboratories) was added (1:300) for 1 hour. Slides were mounted with Vector Shield (Vector laboratories. Burlingame, CA) containing DAPI. Slides were viewed on a fluorescent microscope and positive cells counted. Basal MCs were quantitated by counting rhodamine-labeled (red) dendritic cells overlaying the FITC-labeled (green) Ki-67-staining nuclei in the epidermal basal keratinocytes. The number of basal MCs per $\times 40$ field was counted, along the length of the skin (normally from 15 and 25 fields per skin). MCs co-staining with Ki-67 and Trp1 were counted (at $\times 100$ magnification) if the DAPI-staining MC nucleus was clearly discernable from the surrounding keratinocyte nuclei.

Double-staining for Trp2 and Trp1 was similarly performed, except that after biotinylated donkey anti-rabbit (Jackson ImmunoResearch Laboratories) and Streptavidin-FITC (Jackson ImmunoResearch Laboratories) antibodies were added in the first labeling (Trp2), slides were then blocked with rabbit F_{AB} fragment before the second primary antibody (Trp1) was applied. As a control for crossreaction, the second rabbit primary antibody (Trp2) was left off before the secondary antibody (rhodamine anti-rabbit) was applied. We observed no red MCs that would have indicated crossreactivity between the first primary antibody and final rhodamine-labeled secondary antibody.

DNA repair

Sections were antigen retrieved, and DNA denatured *in situ* by immersion of slides in the following solutions: 50% ethanol for 5 minutes; 30% ethanol/0.02 N HCl for 2 minutes; 0.05 N HCl for 5 minutes; 0.07 N NaOH/70% ethanol for 7 minutes. Sections were blocked for 1 hour with goat-anti-mouse F_{AB} fragment, and then with 1% BSA. The first primary antibody (α-H3 monoclonal, Sigma, Australia) was applied (1:100) overnight at 5 °C. Sections were washed, and biotinylated donkey anti-mouse (Jackson ImmunoResearch Laboratories) was applied (1:300) for 1 hour, followed by FITC-labeled Streptavidin (Jackson ImmunoResearch Laboratories; 1:300) for 1 hour. The subsequent dual-labeling step for Trp1 is described above.

Statistics

Statistical significance was determined for the difference in MC numbers between genotypes using the Mann–Whitney *U*-test. Calculations were performed using the SPSS computer program.

CONFLICT OF INTEREST

The authors state no conflict of interest.

ACKNOWLEDGMENTS

We are grateful to Dr Vince Hearing for PEP1 and PEP8 antibodies, and Dr Marianne Broome-Powell, Dr Mariano Barbacid, and Dr Marcos Malumbres for the *Tpras* and *Cdk4*^{R24C} mice. This study was funded by the Cancer Council of Queensland. NKH is the recipient of a Senior Principal Research Fellowship from the National Health and Medical Research Council of Australia.

SUPPLEMENTARY MATERIAL

Figure S1. DNA repair and MC localization in mouse skin, and UVA lamp spectral characteristics.

REFERENCES

Abdel-Malek ZA, Knittel J, Kadekaro AL, Swope VB, Starner R (2008) The melanocortin 1 receptor and the UV response of human melanocytes-A shift in paradigm. *Photochem Photobiol* 84:501–8

Ackermann J, Frutschi M, Kaloulis K, McKee T, Trumpp A, Beermann F (2005) Metastasizing melanoma formation caused by expression of activated N-RasQ61K on an INK4a-deficient background. *Cancer Res* 65:4005–11

Bardeesy N, Bastian BC, Hezel A, Pinkel D, DePinho RA, Chin L (2001) Dual inactivation of RB and p53 pathways in RAS-induced melanomas. *Mol Cell Biol* 21:2144–53

Beral V, Robinson N (1981) The relationship of malignant melanoma, basal and squamous skin cancers to indoor and outdoor work. *Br J Cancer* 44:886–91

Billingham R, Silvers W (1970) Studies on the migratory behaviour of melanocytes in guinea pig skin. *J Exp Med* 131:101–17

Broome Powell M, Gause PR, Hyman P, Gregus J, Lluria-Prevatt M, Nagle R *et al.* (1999) Induction of melanoma in TPras transgenic mice. *Carcinogenesis* 20:1747–53

Cotter MA, Thomas J, Cassidy P, Robinette K, Jenkins N, Florell S *et al.* (2007) N-acetylcycteine protects melanocytes against oxidative stress/damage and delays age of onset of ultraviolet-induced melanoma in mice. *Cancer Suscep Prev* 13:5952–8

De Fabo EC, Noonan FP, Fears T, Merlino G (2004) Ultraviolet B but not ultraviolet A radiation initiates melanoma. *Cancer Res* 64:6372–6

de Gruijl FR, Sterenborg HJ, Forbes PD, Davies RE, Cole C, Kelfkens G *et al.* (1993) Wavelength dependence of skin cancer induction by ultraviolet irradiation of albino hairless mice. *Cancer Res* 53:53–60

Gerdes J, Lemke H, Baisch H, Wacker HH, Schwab U, Stein H *et al.* (1984) Cell cycle analysis of a cell proliferation-associated human nuclear antigen defined by the monoclonal antibody Ki-67. *J Immunol* 133:1710–5

Grichnik JM, Ali WN, Burch JA, Byers JD, Garcia CA, Clark R *et al.* (1996) KIT reveals a population of precursor melanocytes in human skin. *J Invest Dermatol* 106:967–71

Grichnik JM, Burch JA, Burchette J, Shea CR (1998) The SCF/Kit pathway plays a critical role in control of normal human melanocyte homeostasis. *J Invest Dermatol* 111:233–8

Hacker E, Irwin N, Muller K, Broome-Powell M, Kay G, Hayward N *et al.* (2005) Neonatal ultraviolet radiation exposure is critical for malignant melanoma induction in pigmented *Tpras* transgenic mice. *J Invest Dermatol* 125:1074–7

Hacker E, Muller K, Gabrielli B, Lincon D, Pavey S, Hayward N *et al.* (2006) Spontaneous and UVR-induced multiple metastatic melanoma in *Cdk4*$^{R24C/R24C}$*/TPras* mice. *Cancer Res* 66:2946–52

Hirobe T (1984) Histochemical survey of the distribution of epidermal melanoblasts and melanocytes in the mouse during fetal and postnatal periods. *Anat Rec* 208:589–94

Hirobe T (1988) Developmental changes in the proliferative response of mouse epidermal melanocytes to skin wounding. *Development* 102:567–74

Hirobe T (2004) Role of keratinocyte-derived factors involved in regulating the proliferation and differentiation of mammalian epidermal melanocytes. *Pigment Cell Res* 18:2–12

Horikawa T, Mishima Y, Nishino K, Ichihashi M (1999) Horizontal and vertical pigment spread into surrounding piebald epidermis and hair follicles after suction blister epidermal grafting. *Pigment Cell Res* 12:175–80

Horikawa T, Norris DA, Johnson TW, Zekman T, Dunscomb N, Bennion SD *et al.* (1996) Dopa-negative melanocytes in the outer root sheath of human hair follicles express premelanosomal antigens but not a melanosomal antigen or the melanosome-associated glycoproteins tyrosinase, TRP-1, and TRP-2. *J Invest Dermatol* 106:28–35

Jimbow K, Uesugi T (1982) New melanogenesis and photobiological processes in activation and proliferation of precursor melanocytes after UV-exposure: ultrastructural differentiation of precursor melanocytes from Langerhans cells. *J Invest Dermatol* 78:108–15

Kannan K, Sharpless NE, Xu J, O'Hagan RC, Bosenberg M, Chin L (2003) Components of the Rb pathway are critical targets of UV mutagenesis in a murine melanoma model. *Proc Natl Acad Sci USA* 100:1221–5

Kawaguchi Y, Mori N, Nakayama A (2001) Kit+ melanocytes seem to contribute to melanocyte proliferation after UV exposure as precursor cells. *J Invest Dermatol* 116:920–5

Lin J, Fisher DE (2007) Melanocyte biology and skin pigmentation. *Nature* 445:843–50

Mak SS, Moriyama M, Nishioka E, Osawa M, Nishikawa S (2006) Indispensable role of Bcl2 in the development of the melanocyte stem cell. *Dev Biol* 291:144–53

Nishimura EK, Jordan SA, Oshima H, Yoshida H, Osawa M, Moriyama M *et al.* (2002) Dominant role of the niche in melanocyte stem-cell fate determination. *Nature* 416:854–60

Noonan FP, Recio JA, Takayama H, Duray P, Anver MR, Rush WL *et al.* (2001) Neonatal sunburn and melanoma in mice. *Nature* 413:222–71

Noonan FP, Otsuka T, Bang S, Anver MR, Merlino G (2000) Accelerated ultraviolet radiation-induced carcinogenesis in hepatocyte growth factor/scatter factor transgenic mice. *Cancer Res* 60:3738–43

Peters E, Tobin D, Botchkareva N, Maurer M, Paus R (2002) Migration of melanoblasts into the developing murine hair follicle is accompanied by transient c-kit expression. *J Histochem Cytochem* 50:751–66

Quevedo W, Fleischmann R (1980) Developmental biology of mammalian melanocytes. *J Invest Dermatol* 75:116–20

Quevedo W, McTague C (1963) Genetic influences on the response of mouse melanocytes to ultraviolet light: the melanocyte system of hair-covered skin. *J Exp Zool* 152:159–68

Quevedo W, Szabo G, Virks J, Sinesi S (1965) Melanocyte populations in UV-irradiated human skin. *J Invest Dermatol* 45:295–8

Rane SG, Dubus P, Mettus RV, Galbreath EJ, Boden G, Reddy EP *et al.* (1999) Loss of Cdk4 expression causes insulin-deficient diabetes and Cdk4 activation results in beta-islet cell hyperplasia. *Nat Genet* 22:44–52

Recio A, Noonan FP, Takayama H, Anver MR, Duray P, Rush WL *et al.* (2002) Ink4a/arf deficiency promotes ultraviolet radiation-induced melanomagenesis. *Cancer Res* 62:6724–30

Rivers R (2004) Is there more than one road to melanoma? *Lancet* 363:728–30

Rosdahl I, Szabo G (1978) Mitotic activity of epidermal melanocytes in UV-irradiated mouse skin. *J Invest Dermatol* 70:143–8

Sato T, Kawada A (1972) Mitotic activity of hairless mouse epidermal melanocytes: its role in the increase in melanocytes during ultraviolet radiation. *J Invest Dermatol* 58:71–4

Scott GA, Haake AR (1991) Keratinocytes regulate melanocyte number in human fetal and neonatal skin equivalents. *J Invest Dermatol* 97:776–81

Sharov AA, Li GZ, Palkina TN, Sharova TY, Gilchrest BA, Botchkarev VA (2003) Fas and c-kit are involved in the control of hair follicle melanocyte apoptosis and migration in chemotherapy-induced hair loss. *J Invest Dermatol* 120:27–35

Silvers W, Mintz B (1998) Differences in latency and inducibility of mouse skin melanomas. *Cancer Res* 58:630–2

Staricco R, Miller-Milinska A (1962) Activation of amelanotic melanocytes in the outer root sheath of he hair follicle following ultraviolet rays exposure. *J Invest Dermatol* 39:163–4

Stierner U, Rosdahl I, Augustsson A, Kagedal B (1989) UVB irradiation induces melanocyte increase in both exposed and shielded human skin. *J Invest Dermatol* 92:561–4

Tron VA, Trotter MJ, Ishikawa T, Ho VC, Li G (1998) p53-dependent regulation of nucleotide excision repair in murine epidermis *in vivo*. *J Cutan Med Surg* 3:16–20

van Schanke A, Jongsma MJ, Bisschop R, van Venrooij GM, Rebel H, de Gruijl FR *et al* (2005) Single UVB overexposure stimulates melanocyte proliferation in murine skin, in contrast to fractionated or UVA-1 exposure. *J Invest Dermatol* 124:241–7

Walker GJ, Hayward NK (2002) Pathways to melanoma development: lessons from the mouse. *J Invest Dermatol* 119:783–92

Whiteman DC, Stickley M, Watt P, Hughes MC, Davis M, Green A (2006) Anatomic site, sun exposure, and risk of cutaneous melanoma. *J Clin Oncol* 24:3172–7

Whiteman DC, Watt P, Purdie DM, Hughes MC, Hayward NK, Green AC (2003) Melanocytic nevi, solar keratoses, and divergent pathways to cutaneous melanoma. *J Natl Cancer Inst* 95:806–12

Wolnicka-Glubisz A, Damsker J, Constant S, Corn S, De Fabo E, Noonan F (2007) Deficient inflammatory response to UV radiation in neonatal mice. *J Leukoc Biol* 81:1352–61

Wolnicka-Glubisz A, Noonan FP (2006) Neonatal susceptibility to UV induced cutaneous malignant melanoma in a mouse model. *Photochem Photobiol Sci* 5:254–60

Yonetani S, Moriyama M, Nishigori C, Osawa M, Nishikawa S (2008) *In vitro* expansion of immature melanoblasts and their ability to repopulate melanocyte stem cells in the hair follicle. *J Invest Dermatol* 128: 408–20